

NASA CR-54474
65-1E5-MHDIN-R1

SEMIANNUAL REPORT

ELECTRON COLLISION CROSS SECTIONS IN METAL VAPORS

By

J. F. Nolan and W. S. Emmerich

prepared for

NATIONAL AERONAUTICS AND SPACE ADMINISTRATION

August 19, 1965

Contract NAS3-7100

Technical Management
NASA Lewis Research Center
Cleveland, Ohio
Spacecraft Technology Division
N. J. Stevens

WESTINGHOUSE RESEARCH LABORATORIES
Beulah Road, Churchill Borough
Pittsburgh, Pennsylvania 15235

ELECTRON COLLISION CROSS SECTIONS IN METAL VAPORS

By

J. F. Nolan and W. S. Emmerich

ABSTRACT

10670

The Townsend α coefficient has been measured in cesium-helium mixtures as a function of E/p , the ratio of electric field to total pressure, and $N_{\text{Cs}}/N_{\text{He}}$, the ratio of cesium to helium density. By comparing the observed α with that obtained from a numerical solution of the Boltzmann equation using an assumed cesium excitation cross section, one obtains a cross section consistent with these measurements and with previous measurements of the cesium ionization cross section. An excitation cross section with a peak value of $1.15 \times 10^{-14} \text{ cm}^2$ at 8 eV gives good agreement with experiment.

Author

ELECTRON COLLISION CROSS SECTIONS IN METAL VAPORS

By

J. F. Nolan and W. S. Emmerich

Westinghouse Research Laboratories

SUMMARY

Prebreakdown ionization build-up has been studied in cesium-helium mixtures of various concentrations. The Townsend α coefficient has been obtained as a function of E/p , the ratio of electric field to total pressure, and $N_{\text{Cs}}/N_{\text{He}}$, the ratio of cesium to helium density. For $N_{\text{Cs}}/N_{\text{He}} \sim 10^{-5}$ the measured values for the α coefficient are more than an order of magnitude larger than the previously measured values in pure helium in the E/p_{300} range from 2.0 to 4.0 volt/cm-Torr (where p_{300} is the total pressure normalized to a temperature of 300°K). Analysis of these measurements shows that the increased ionization is produced mainly by Penning effect collisions; i.e. electrons excite helium atoms to a metastable state and these metastable atoms ionize cesium atoms on collision. At larger density ratios ($N_{\text{Cs}}/N_{\text{He}} \sim 10^{-4}$) direct electron ionization of cesium becomes the dominant ionization mechanism for $E/p_{300} < 2.5$ volts/cm-Torr. By comparing the measured α with that obtained from a numerical solution of the Boltzmann equation using an assumed excitation cross section, one obtains a cross section consistent with the present α measurements and with previous measurements of the cesium ionization cross section. An excitation cross section with a peak value of $1.15 \times 10^{-14} \text{ cm}^2$ at 8 eV gives good agreement with experiment.

INTRODUCTION

Electron swarm techniques for studying elastic and inelastic cross sections for electrons in gases have been developed in recent years and applied successfully to the noble gases¹⁻³ and to certain diatomic molecules⁴⁻⁶. In addition, preliminary experiments have indicated that similar techniques can be employed to obtain cross sections in metallic vapors, particularly in cesium, by making measurements in a mixture of cesium and a noble gas⁷. During the first six months of the present program, measurements of the Townsend α coefficient have been carried out in cesium-helium mixtures of various density ratios, extending considerably the previously available data on the cross section for electron excitation of cesium.

The present technique involves the measurement of the Townsend ionization coefficient as a function of E/p , and also as a function of $N_{\text{Cs}}/N_{\text{He}}$. The data is analyzed to give a collision cross section by a process involving a numerical solution of the Boltzmann transport equation which makes no a priori assumptions about the shape of the electron energy distribution function. The measurements of the Townsend α coefficient presented here are analyzed to give the total cross section for electron excitation of cesium from threshold to 10 eV. The cesium excitation cross section obtained in the present work is compared with estimates based on previous experimental measurements, and with several theoretical calculations.

APPARATUS

The apparatus used for these measurements is shown in Figure 1 with the main oven in place, and in Figure 2 with the oven removed; Figure 3 shows a schematic drawing of the vacuum system. The portion of the vacuum system inside the oven is constructed of stainless steel; the section outside the oven is constructed mainly of glass. The measurements are made in the drift tube shown in Figure 3; this will be described in more detail below. The temperature of the main oven for these experiments was in the range 250-300°C. The cesium was contained in a U-tube in a separate oven where its temperature could be controlled independently of the main oven. The main oven was maintained at a temperature higher than that of the Cs reservoir oven to prevent cesium from condensing in the drift tube. When the by-pass valve is closed (Fig. 3), the Cs vapor pressure in the drift tube at equilibrium corresponds to the vapor pressure at the reservoir temperature provided the collision mean free path is short compared to the dimensions of the connecting tubing, as was the case for all of the measurements reported here.

To the glass portion of the system is connected a Bayard-Alpert ionization gauge for measuring the residual vacuum pressure, a null-indicating diaphragm manometer for measuring high pressures, and a supply of reagent grade helium. Before the cesium ampule was broken the pressure in the system was about 5×10^{-9} Torr, with a rate of rise of 2×10^{-9} Torr/min. with the system isolated from the pumps. The null-indicating diaphragm manometer is an improved version of the one described by Alpert⁸. For the high total pressures used in these measurements (< 300 Torr) it is capable of measuring the pressure with an accuracy better than 1%. Since the ratio

of Cs to He pressure was always small (10^{-4} or less) the total pressure was equal to the He pressure to a very good approximation. The cesium vapor pressure was calculated from the expression given by Taylor and Langmuir⁹

$$\log_{10} p = 11.0531 - \frac{4041}{T} - 1.35 \log_{10} T \quad (1)$$

where p is the vapor pressure in Torr and T is the temperature of the Cs reservoir in $^{\circ}\text{K}$.

Figure 4 shows a photograph of the drift tube with the vacuum jacket removed. The main elements are two parallel plate electrodes made of advance (nickel-copper alloy). One of the electrodes has a guard ring around the outside, as shown in Figure 5, to insure that the applied electric field is uniform in the central region. Currents are measured to the central disc. The spacing between the two electrodes is variable between 0.05 and 1 cm. through the bellows arrangement shown in Figure 4. The electrode spacing was calibrated as a function of the micrometer driver reading using a cathetometer with the drift tube encased in a glass envelope and evacuated to the operating pressure.

The circuitry used in the measurements of the Townsend α coefficient consists of a regulated dc voltage supply connected between ground and one of the electrodes (the unguarded one) and a nanovoltmeter connected across a variable load resistor at the other electrode. This latter combination was used to measure the current to the central disc. The current was in the range 10^{-10} to 10^{-6} amperes. The leakage resistance was of the order of 10^4 ohms, so that a conventional low current ammeter could not be used to measure the current, since the input impedance of such an instrument is large compared to the leakage resistance.

METHOD

For a uniform dc electric field applied between parallel plates, the prebreakdown current as a function of distance is given by¹⁰

$$I(x) = \frac{I_0 \exp \alpha (x - x_0)}{1 - \gamma (\exp [\alpha (x - x_0)] - 1)} \quad (2)$$

where I_0 is the initial current at $x = 0$, x is the distance from the electrode which acts as the current source, x_0 is related to the distance which electrons must travel before an equilibrium velocity distribution is attained, γ is a generalized coefficient referring to electron production due to secondary processes, and α is the Townsend α coefficient. x_0 is related to the electron mean free path and, for the high pressures used in the present measurements, may be safely taken as zero. If, in addition, secondary processes are not important, the above reduces to

$$I(x) = I_0 \exp (\alpha x) \quad (3)$$

so that α may be obtained by measuring I/I_0 as a function of x . Experimentally, one may determine whether or not secondary processes are important by plotting $\ln (I/I_0)$ vs. x . If secondary effects are important, the curves will bend upward; if not, straight lines will be obtained.

In the present case the initial current is supplied by thermionic emission from the cesium coated electrodes at the equilibrium temperature of the tube ($\sim 300^\circ\text{C}$). Since both electrodes are emitting, the prebreakdown current may be observed in either direction simply by reversing the polarity of the applied electric field. The initial current, I_0 , cannot be measured directly in most cases, since at the high pressures used for the measurements there is a significant amount of back diffusion; i.e. some of the emitted

electrons undergo collisions with the gas molecules in the immediate vicinity of the emitting surface and are reflected back to it. As the applied electric field is increased, back diffusion becomes less important, but ordinarily ionization build-up sets in before the initial current reaches I_0 ; i.e., ordinarily there is no definite plateau in the I vs. E curve for a given spacing. One can get around this difficulty by measuring I/I_c where I_c is the current at some low value of E/p where there is no ionization build-up. I_c is some constant fraction of I_0 , so that α may be obtained from graphs of $\ln(I/I_c)$ vs. x .¹¹ It should be noted that the only reason for measuring I_c is to guard against the possibility that I_0 may change somewhat with time; if I_0 does not change, α may be obtained by simply measuring I as a function of distance. In the present measurements it was found that there was no significant short term change in I_c at a given E/p .

The procedure used in taking measurements was to first measure the current at a given spacing as the applied voltage was varied from zero up to near the breakdown voltage; then change the spacing and repeat. When the data obtained at several spacings were plotted vs. E/p , the resulting curves were coincident for low E/p . This allowed one to pick a value of E/p appropriate for measuring I_c ; i.e. a value low enough so that there was no ionization build-up. In all cases it was found that there was no ionization build-up at $E/p_{300} = 1.0$ volt/cm-Torr (where p_{300} is the total pressure normalized to a temperature of 300°K), and I_c was measured at this value of E/p_{300} . Then the ratio of I/I_c was measured as a function of the spacing, where I is the current at some higher value of E/p_{300} , where ionization build-up occurs. Sample curves of I/I_c vs x for several values of E/p_{300} are shown in Figure 6. This data was obtained with a total normalized pressure of $p_{300} = 260$ Torr and cesium to helium density ratio of

2.72×10^{-5} . It will be observed that the curves are linear, indicating that secondary processes are not important, so that α may be obtained from the slope. The $\ln(I/I_c)$ vs. x curves were found to be linear in all cases except for some measurements made at high values of E/p_{300} ($E/p_{300} \sim 4.0$ volts/cm - Torr), where some curvature was observed. As a check, the data was also reduced using a method due to Gosseries¹² which gives an unambiguous value of α regardless of the magnitude of γ . The values of α obtained in this analysis agreed with those obtained from the slope of $\ln(I/I_c)$ vs x curves to within a few percent.

The procedure used in obtaining a cesium-helium mixture was to admit helium to the desired total pressure with the cesium reservoir cooled, and then close the by-pass valve (Fig. 3) and raise the temperature of the cesium reservoir to give the desired cesium vapor pressure. Measurements of α as a function of time after closing the by-pass valve showed that considerable time was required for the mixture to reach equilibrium. The values of α obtained at a given E/p_{300} increased at first and did not become constant with time until 2 to 3 days after the by-pass valve was closed. Once equilibrium was attained the value of α measured was constant with time to within experimental error for as long as measurements were made on a given mixture (up to two weeks). This long time required to reach an equilibrium mixture had been observed in previous measurements of drift velocity in cesium-argon mixtures in the same system,⁷ and is presumed to be due to a combination of diffusion and wall coating effects. The path from the cesium reservoir to the drift tube is relatively long with a small diameter. The results presented here are the long time, equilibrium measurements of the Townsend α coefficient.

RESULTS

The Townsend α coefficient was measured as a function of E/p_{300} in cesium-helium mixtures with several different values of $N_{\text{Cs}}/N_{\text{He}}$. Figure 7 shows the results obtained for α/p_{300} vs. E/p_{300} with $N_{\text{Cs}}/N_{\text{He}} = 2.72 \times 10^{-5}$. Also shown for comparison in Figure 7 is α/p_{300} for pure helium, taken from Chanin and Rork.¹³ Although the values of α/p_{300} obtained for this mixture are considerably larger than the pure helium values, analysis of the data (discussed in the following section) showed that this enhancement was due mainly to the Penning effect rather than to direct electron ionization of cesium.

Figure 8 shows the results of measurements of α/p_{300} under conditions where the main ionization mechanism at low E/p_{300} is direct ionization of cesium. The density ratio in this case is $N_{\text{Cs}}/N_{\text{He}} = 9.0 \times 10^{-5}$. Also shown in Figure 8 are curves which give the α values calculated on the basis of an assumed Cs excitation cross section. These calculations are discussed in the next section.

A qualitative explanation of the results of these measurements is as follows: At low density ratios, electron-cesium collisions are so infrequent that they have no significant effect on α . As E/p is increased the electron distribution function extends to higher energies so that there is significant excitation of helium. Metastable helium atoms can then ionize cesium atoms on collision (Penning effect), causing a higher α than would be the case in pure helium. As the cesium to helium density ratio is increased, direct ionization of cesium by electrons becomes a competing process in producing ion pairs. Since the cesium ionization threshold (3.89 eV) is considerably below the helium excitation threshold (19.8 eV), the direct

ionization process will begin to contribute to the total α at a lower E/p than the Penning effect. There is a range of E/p in which the contribution of the Penning effect to the total α is negligible. In this range of E/p the Townsend α coefficient will depend only on the cesium excitation and ionization cross sections and on the helium momentum transfer cross section. Since the helium momentum transfer cross section and the cesium ionization cross section are known, the measurements may be analyzed to give the total cesium excitation cross section. The method of analysis is discussed in the next section.

ANALYSIS OF DATA

In order to obtain the cesium excitation cross section as a function of electron energy from the Townsend α coefficient as a function of E/p , it is necessary to know the electron energy distribution function. In general, however, one does not know the shape of the distribution function a priori, since this depends in part upon the cross section one is attempting to find. The assumption of a Maxwellian or Druyvesteynian shape is not justified under the conditions of the present measurements. The procedure followed is to assume an excitation cross section, with the proper threshold, as a function of energy and to use this cross section in obtaining a numerical solution of the Boltzmann equation. This gives the distribution function appropriate to the assumed cross section, so that the Townsend α coefficient can then be calculated as a function of E/p . This calculated α coefficient is then compared to the experimental values, and the input cross section is adjusted in magnitude and shape until the calculated and experimental α coefficients agree. This allows one to obtain a cross section which is consistent with the experimental results. The final cross section obtained in this way is not unique in that rapid changes with energy in the cross section curve will be at least partially averaged out because of the relatively large spread in the electron energy distribution.

The analysis of the data in the present work is similar to that used by Frost and Phelps⁴ and by Engelhardt and Phelps⁵ and will only be outlined here. The basis of the analysis is the Boltzmann equation for the distribution function of electrons in the gas mixture, which we write in the form

$$\begin{aligned}
 & \frac{d}{d\epsilon} \left[\frac{e^2 E^2 \epsilon}{3 (N_{\text{He}} Q_{\text{He}} + N_{\text{Cs}} Q_{\text{Cs}})} \frac{df}{d\epsilon} \right] \\
 & + 2m \frac{d}{d\epsilon} \left[\epsilon^2 \left(\frac{N_{\text{He}} Q_{\text{He}}}{M_{\text{He}}} + \frac{N_{\text{Cs}} Q_{\text{Cs}}}{M_{\text{Cs}}} \right) \left(f + kT \frac{df}{d\epsilon} \right) \right] \\
 & + \sum_j \left[(\epsilon + \epsilon_j) f(\epsilon + \epsilon_j) N_{\text{Cs}} Q_{j\text{Cs}}(\epsilon + \epsilon_j) - \epsilon f(\epsilon) N_{\text{Cs}} Q_{j\text{Cs}}(\epsilon) \right] \\
 & + \sum_j \left[(\epsilon + \epsilon_j) f(\epsilon + \epsilon_j) N_{\text{He}} Q_{j\text{He}}(\epsilon + \epsilon_j) - \epsilon f(\epsilon) N_{\text{He}} Q_{j\text{He}}(\epsilon) \right] = 0
 \end{aligned} \tag{4}$$

where ϵ is the electron energy ($= 1/2 mv^2$, where v is the electron speed), e is the electron charge, E the applied electric field, N_{He} and N_{Cs} the densities of helium and cesium, Q_{He} and Q_{Cs} the energy-dependent momentum-transfer cross sections for helium and cesium, $f(\epsilon)$ is the steady state electron energy distribution function, m is the electron mass, M_{He} the mass of a helium atom, M_{Cs} the mass of a cesium atom, k is Boltzmann's constant, T is the gas temperature, and Q_j represents the cross section for the j th inelastic process

involving an electron energy loss ϵ_j . The distribution function is normalized by

$$\int_0^{\infty} \epsilon^{1/2} f(\epsilon) d\epsilon = 1 \quad (5)$$

The terms of Eq. (4) may be associated with a gain or loss of energy due to one of the processes being considered. The first term represents the effect of energy input to the electrons from the applied field, the second term energy loss and gain in elastic collisions, the third term energy loss in inelastic collisions with cesium, and the fourth term energy loss in inelastic collisions with helium. Terms involving collisions of the second kind are not included, since they are not important for the relatively high energies considered here.

The helium momentum transfer cross section used in the calculations was taken from Frost and Phelps.³ The momentum transfer cross section for cesium was taken from Brude¹⁴ at high energies (above 0.5 eV) and from Frost¹⁵ at low energies. Although there is some uncertainty in the low energy values of Q_{Cs} , this is not important in the present analysis, since the contribution of cesium to the effective momentum transfer cross section for the mixture is negligible. This may be seen by noting that in Eq. (4) Q_{Cs} appears multiplied by N_{Cs} and added to a similar product term for helium. Since for the cases considered here N_{Cs} is always less than $10^{-4} N_{He}$, and since Q_{Cs} never gets as large as $10^2 Q_{He}$ in the appropriate energy range, the contribution of cesium to the effective momentum transfer cross section is less than 1%.

Four inelastic cross sections are used in Eq. (4): excitation and ionization cross sections for cesium and helium. The cesium ionization cross section has a shape based on the measurements of Tate and Smith¹⁶ and a magnitude of $1.0 \times 10^{-15} \text{ cm}^2$ at the peak of the cross section. The magnitude of the peak value chosen is a compromise between the peak values reported by Brink¹⁷ ($1.12 \times 10^{-15} \text{ cm}^2$) and by McFarland and Kinney¹⁸ ($0.94 \times 10^{-15} \text{ cm}^2$). The helium excitation cross section is based on the measurements of Maier-Leibnitz¹⁹, and the helium ionization cross section is taken from Smith.²⁰ The cesium excitation cross section is the one unknown cross section which enters into Eq. (4). It is therefore possible to obtain by numerical methods a curve of this cross section versus energy which is consistent with the experimental measurements of α and with the other known cross sections.

Eq. (4) is solved numerically to obtain the electron energy distribution function, $f(\epsilon)$, using a trial excitation cross section with correct threshold. Then, using this distribution function, the Townsend α coefficient is calculated from the relation

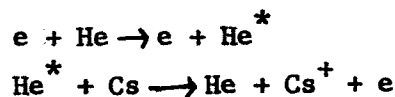
$$\alpha = \frac{N}{w} \sqrt{\frac{2}{m}} \int_0^{\infty} \epsilon f(\epsilon) Q_i(\epsilon) d\epsilon \quad (6)$$

where $Q_i(\epsilon)$ is the cesium ionization cross section, N is the total gas density, and w is the electron drift velocity, given by

$$w = - \frac{Ee}{2} \sqrt{\frac{2}{m}} \int_0^{\infty} \frac{\epsilon}{(N_{\text{He}} Q_{\text{He}} + N_{\text{Cs}} Q_{\text{Cs}})} \frac{df}{d\epsilon} d\epsilon \quad (7)$$

where the Q 's in Eq. (7) refer to momentum transfer cross sections. The values of α calculated from Eq. (6) are then compared with the measured values, and the magnitude and shape of the assumed cesium excitation cross section are varied until good agreement is obtained between the calculated and measured values. Although only the cesium ionization cross section appears explicitly in Eq. (6), α depends quite strongly on the cesium excitation cross section, because of the dependence of the distribution function on the excitation cross section. In the present case, the calculated values of α are more sensitive to changes in the cesium excitation cross section than to changes in the ionization cross section.

The cesium excitation cross section which gives best agreement between the calculated and measured α is shown in Fig. 9. The peak magnitude is $1.15 \times 10^{-14} \text{ cm}^2$ at 8 eV. The initial slope of the cross section for energies less than 2 eV is in good agreement with the previously determined value of $7.1 \times 10^{-15} \text{ cm}^2 \text{ eV}^{-1}$. A comparison of the values of α/p_{300} calculated using this cross section with the measured values is shown in Figure 8 for $N_{\text{Cs}}/N_{\text{He}} = 9.0 \times 10^{-5}$. For $E/p_{300} < 2.5 \frac{\text{volts}}{\text{cm-Torr}}$ the Penning effect contribution is negligible and all of the ionization is produced by the direct process. The calculation of the contribution due to the Penning effect shown in Fig. 8 for the higher values of E/p_{300} is based on the assumption that all of the helium metastables formed are destroyed in Penning effect collision with cesium. That is, we have the two step process



and it is assumed that no other mechanism contributes significantly to the destruction of helium metastables. The fact that the sum of the Penning

effect ionization calculated on this basis and the direct cesium ionization is in good agreement with the experimental results in the higher E/p range lends support to this assumption.

Examples of calculated distribution functions are shown in Figure 10 for two values of E/p_{300} . Also shown for comparison is a Maxwellian distribution with a peak energy corresponding to that of the calculated distribution function at $E/p_{300} = 3.0$ volts/cm-Torr. It will be seen that the actual distribution function falls off more rapidly with energy than a Maxwellian.

The sensitivity of the calculated α to the assumed Cs excitation cross section is quite good, as illustrated in Fig. 11. Here the solid curve is the α calculated using the best excitation cross section (i.e. the curve in Fig. 9) while the dotted curve shows the results of a calculation using one of the earlier trial cross sections which was only 20% smaller than the final value (the peak magnitude for this cross section was 0.95×10^{-14} cm², and the shape was very nearly the same as the final shape). Since the dotted curve is clearly in disagreement with the measurements, we may conclude that the best cross section may be obtained with a sensitivity of better than 20%. The experimental values were reproducible to $\pm 5\%$, and their absolute accuracy is believed to be within $\pm 10\%$. Perhaps the greatest uncertainty in the present value for the cesium excitation cross section lies in the uncertainty associated with the magnitude taken for the cesium ionization cross section. If this cross section is correct to within 20%, as it appears to be considering the agreement between Brink and McFarland and Kinney, then the present value for the cesium excitation cross section should also be correct to within 20%.

It has been previously mentioned that the present method of obtaining cross sections is not sensitive to rapid changes of the cross section with energy. Thus, any sharp resonances which may be present in the cross section will not be observed using an electron swarm technique such as that used here. It is therefore possible that the cross section curve shown in Fig. 9 represents a smoothed-out average of the true cross section, if the true cross section contains some rapid energy variations.

DISCUSSION

Although measurements of total, momentum transfer, and ionization cross sections in cesium have been reported in the literature at various times, no absolute values for excitation cross sections have yet been published. Measurements of the excitation function for some of the spectral lines of cesium have been reported by Bogdanova²¹ and by Zapesochnyi and Shimon.²² The latter authors give the shape of the excitation function for one of the resonance lines, but do not give absolute values for the cross section. A comparison of the cross section obtained in the present work with the Zapesochnyi and Shimon excitation function for resonance radiation is of interest since it provides a check on the proposal⁷ that excitation to the resonance states accounts for most of the total excitation; i.e., excitation to states higher than the resonance states is relatively unimportant. If this idea is correct, the shape of the total cross section should be roughly the same as that for resonance excitation. Such a comparison is shown in Fig. 12 and it is seen that the shapes of the two curves are roughly the same. The Zapesochnyi and Shimon curve is normalized to the present curve at 8 eV.

Recent drift velocity measurements at this laboratory gave an absolute value of $7.1 \times 10^{-15} \text{ cm}^2/\text{eV}$ for the initial slope of the cesium excitation cross section in the threshold region.⁷ An estimate of the cross section at higher energies was obtained by normalizing the Zapesochnyi and Shimon resonance curve to the absolute value obtained for the initial slope. The cross section estimated in this way was about 20% smaller than that reported here around the peak of the cross section; the present results agree very well with the previous value found for the initial slope.

Theoretical calculations of the cross section for 6S-6P excitation in cesium have been reported by Hansen²³, Witting,²⁴ and by Vainshtein, et.al.²⁵ Although the present experiment measures the total excitation cross section rather than only 6S-6P excitation, a comparison of the present results with these calculations is significant since, as has been pointed out, the cross section for excitation to states higher than the 6P states is expected to be small. Such a comparison is shown in Fig. 13. The calculated 6S-6P cross sections are somewhat lower than the measured total cross section, as expected, but the fact that the calculations of Hansen and of Witting are within 20% of the measured value is consistent with the idea that 6S-6P resonance excitation accounts for most of the total excitation cross section.

The results presented here were obtained in mixtures with cesium to helium density ratios of 10^{-4} or less. It has been possible to use these measurements to get the cesium excitation cross section because in the E/p_{300} range from about 1 to 3 volts/cm-Torr the dominant inelastic collision processes are excitation and ionization of cesium atoms by electrons; elastic collisions of electrons with cesium are negligible for these density ratios. In order to obtain measurements which can be used to obtain the

cesium momentum transfer cross section, it is necessary to go to density ratios about two orders of magnitude higher. A few drift velocity measurements have been made in mixtures with a density ratio approaching 10^{-2} . The drift velocity was found to be somewhat lower than the known drift velocity in pure helium, indicating that electron-cesium elastic collisions were appreciable. It has not been possible to get a reliable cesium momentum transfer cross section from these measurements, however, since only a small amount of data could be obtained, due to deterioration of the insulators. The system is presently being modified to improve the insulation and to reduce the time required for a mixture to reach equilibrium concentration.

ACKNOWLEDGEMENTS

The authors wish to express their appreciation to A.V. Phelps for many valuable discussions.

REFERENCES

1. J. L. Pack and A. V. Phelps, Phys. Rev. 121, 798 (1961)
2. J. L. Pack, R. E. Voshall, and A. V. Phelps, Phys. Rev. 127, 2084 (1962)
3. L. S. Frost and A. V. Phelps, Phys. Rev. 136, A1538 (1965).
4. L. S. Frost and A. V. Phelps, Phys. Rev. 127, 1621 (1962).
5. A. G. Engelhardt and A. V. Phelps, Phys. Rev. 131, 2115 (1963)
6. A. G. Engelhardt and A. V. Phelps, Phys. Rev. 135, A1566 (1964)
7. J. F. Nolan and A. V. Phelps, Westinghouse Scientific Paper 65-9E3-113-P1, April 15, 1965 (To be published).
8. D. Alpert, C. G. Matland and A. O. McCoubrey, Rev. Sci. Instr. 22, 370 (1951)
9. J. B. Taylor and I. Langmuir, Phys. Rev. 51, 753 (1937).
10. A. von Engle, Handbuch Der Physik, Edited by S. Flugge (Springer-Verlag, Berlin, 1956), Vol. XXI, p. 504.
11. For a discussion of the measurement of I_o and I_c , see R. W. Crompton, J. Dutton, and S. C. Haydon, Proc. Phys. Soc. (London), B69, 2 (1956).
12. A. Gosseries, Physica 6, 458 (1939).
13. L. M. Chanin and G. D. Rork, Phys. Rev. 133, 1005 (1964).
14. R. B. Brode, Phys. Rev. 34, 673 (1929).
15. L. S. Frost, J. Appl. Phys. 32, 2029 (1961).
16. J. T. Tate and P. T. Smith, Phys. Rev. 46, 773 (1934).
17. G. O. Brink, Phys. Rev. 134, A345 (1964).
18. R. H. McFarland and J. D. Kinney, Phys. Rev. 137, A1058 (1965).
19. H. Maier-Leibnitz, Z. Phys. 95 (1935).
20. P. T. Smith, Phys. Rev. 36, 1293 (1930).
21. I. P. Bogdanova, Bull. Acad. Sci. USSR, Phys. Ser. 24, 958 (1960).
22. I. P. Zapesochnyi and L. L. Shimon, Opt. Spectry (USSR) 16, 504 (1964).
23. L. K. Hansen, J. Appl. Phys. 35, 254 (1964).
24. H. L. Witting, Quarterly Progress Report No. 70, Research Laboratory of Electronics, MIT (July 1963), P. 153; see Also H. L. Witting and E. P. Gyftopoulos, J. Appl. Phys. 36, 1328 (1965).
25. L. Vainshtein, V. Opyktin and L. Presnyakov, Zhur. Eksp. i. Teoret. Fiz. 47, 2306 (1964).

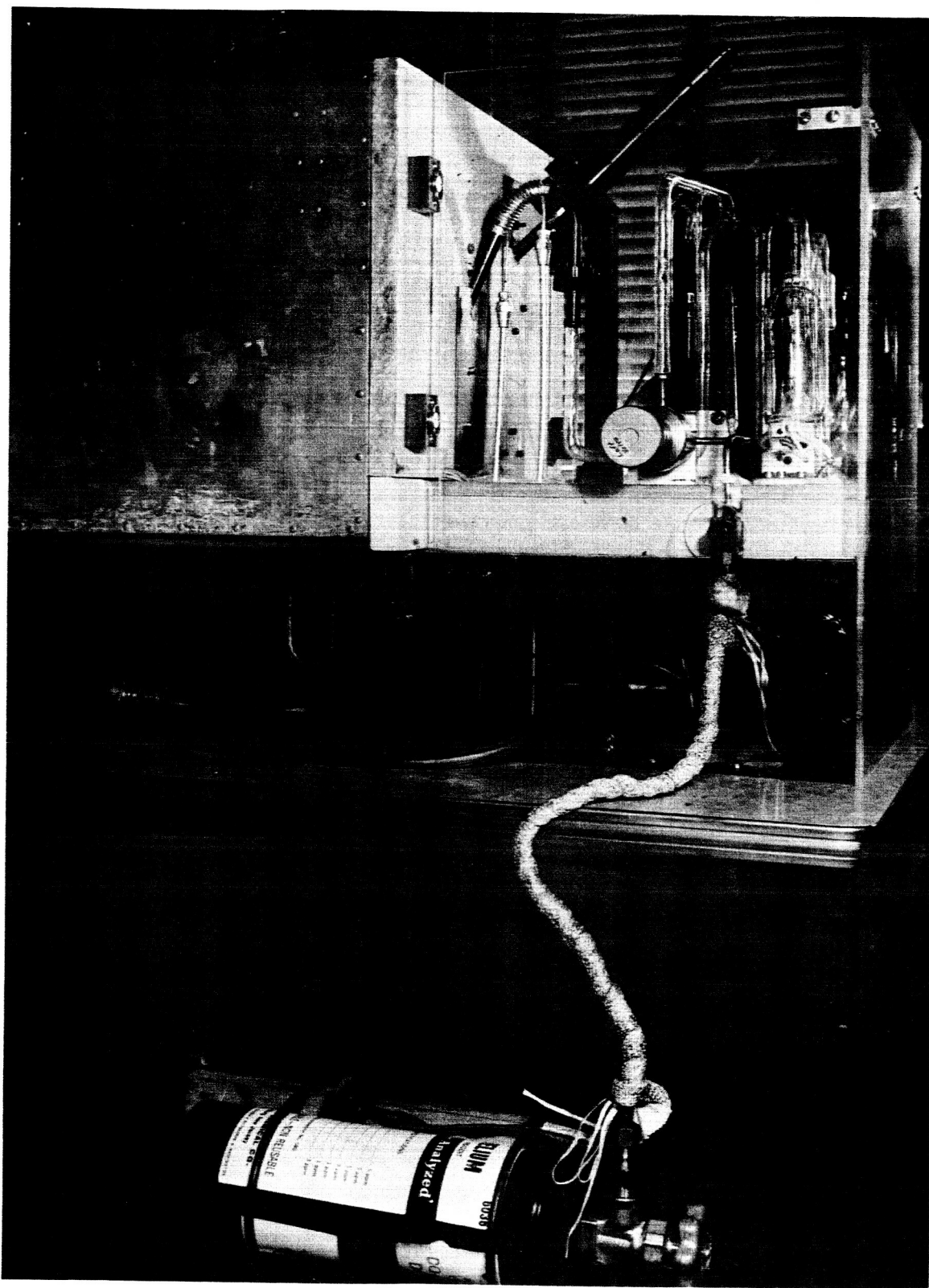


Figure 1 Photograph of apparatus with main oven in place. The U-tube, which acts as the Cs reservoir, may be seen extending below the main oven. The Cs reservoir oven was not in place when the photograph was taken.

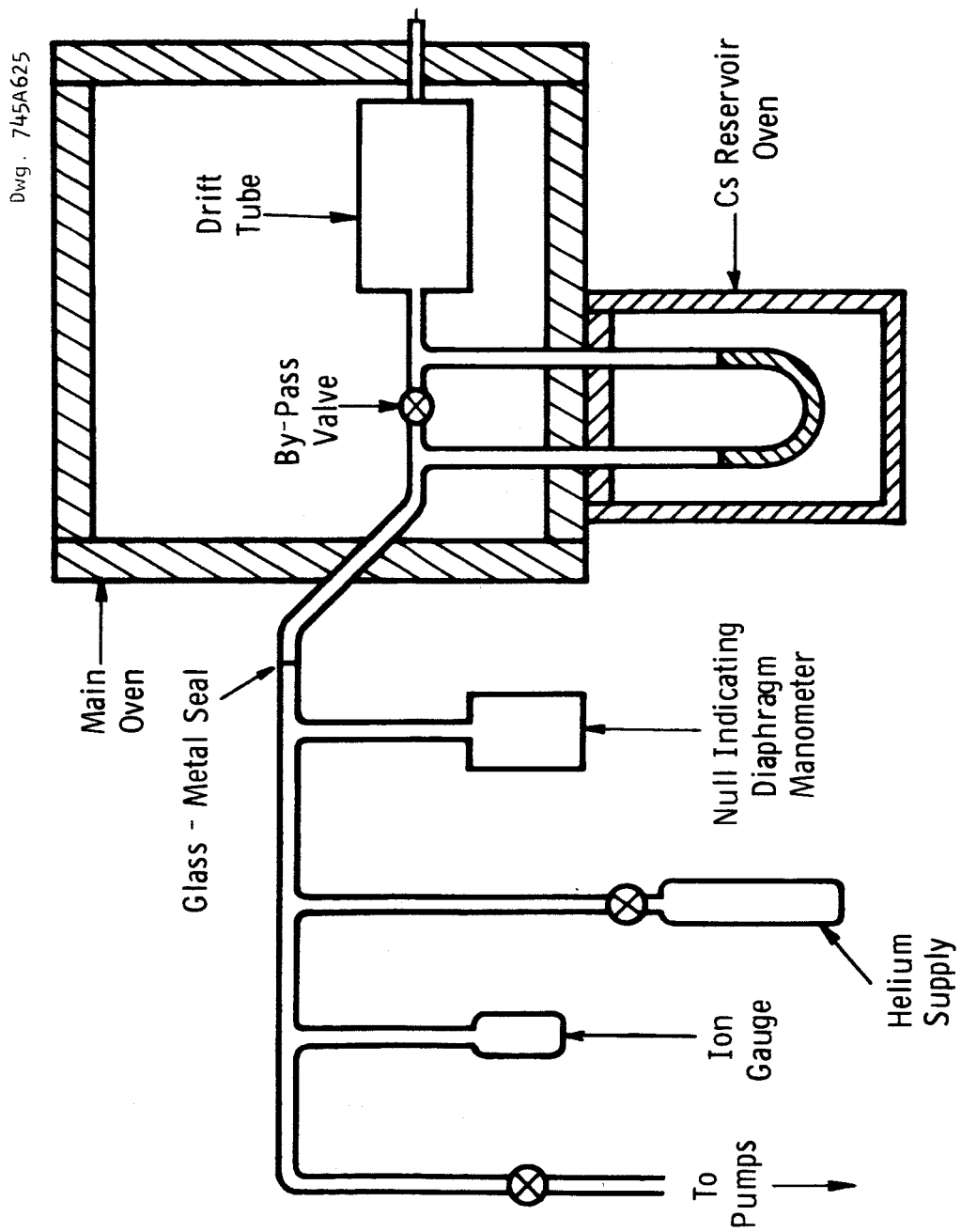


Figure 3 Schematic diagram of vacuum system.

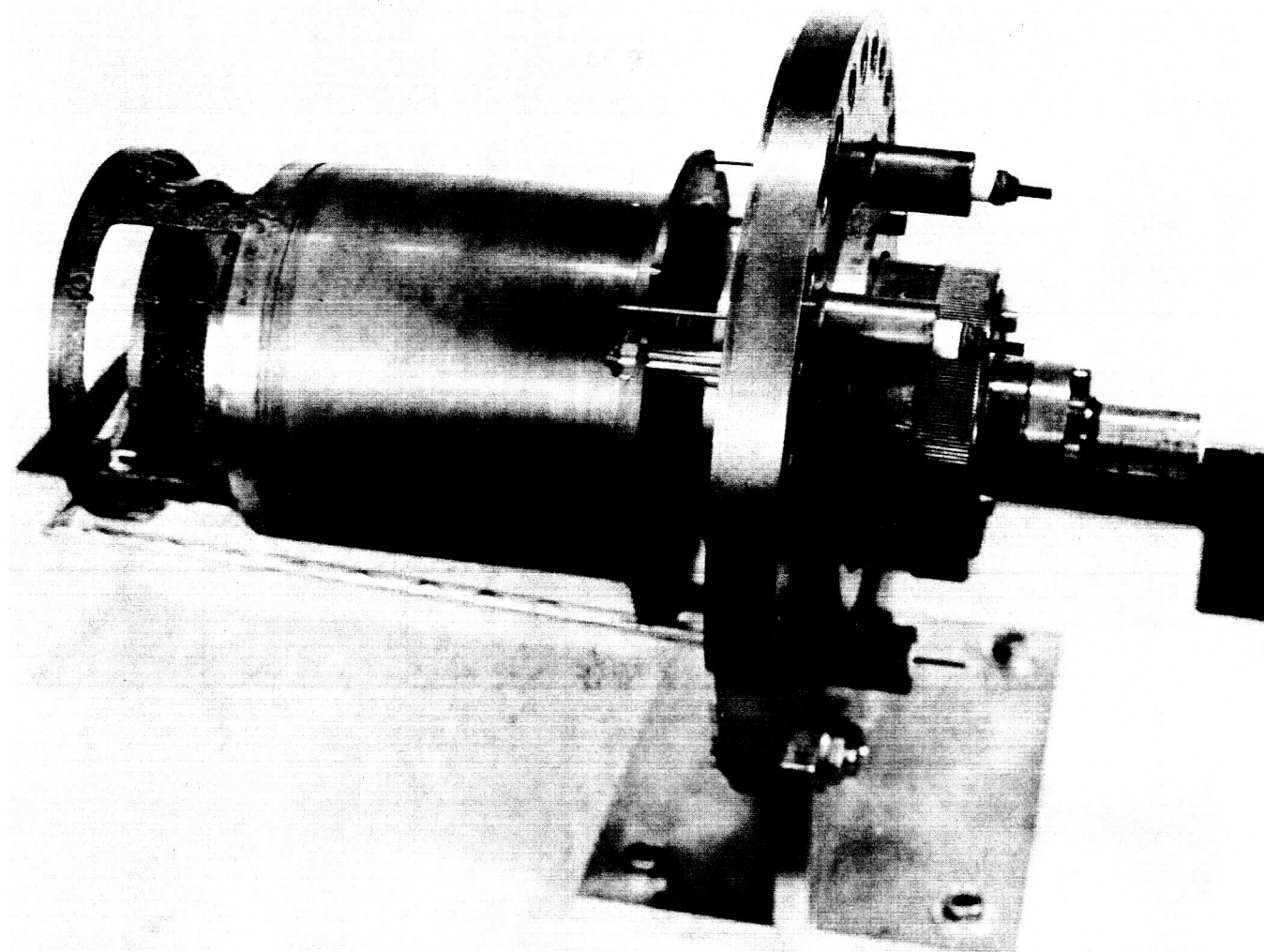


Figure 4 Drift tube with vacuum jacket removed.



Figure 5 Detail of electrode region of drift tube, showing split structure of electrode. Currents are measured to the central disc; the outer guard ring is used to maintain uniformity of the applied electric field in the central region.

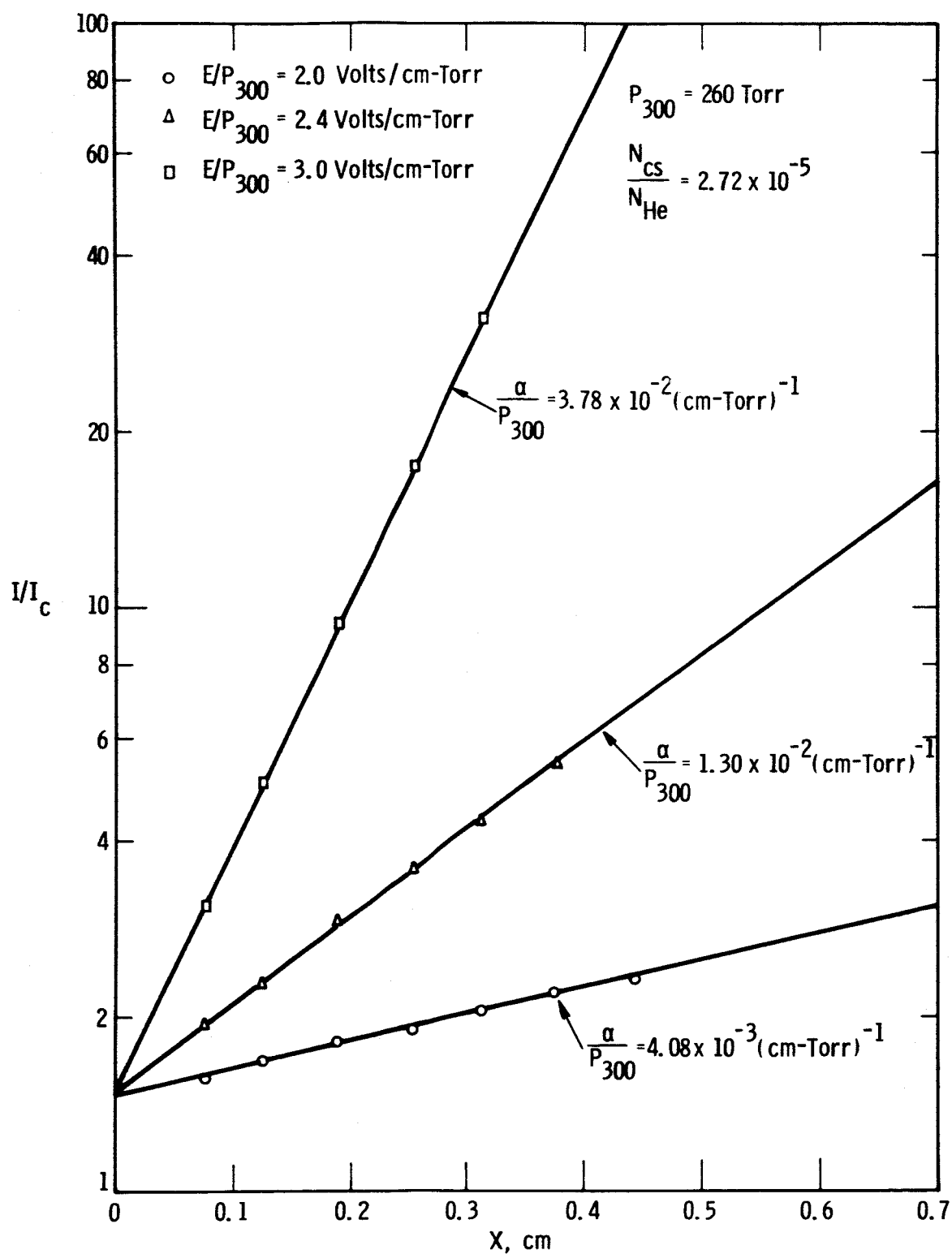


Figure 6 Sample curves of $\ln(I/I_c)$ vs. electrode spacing.

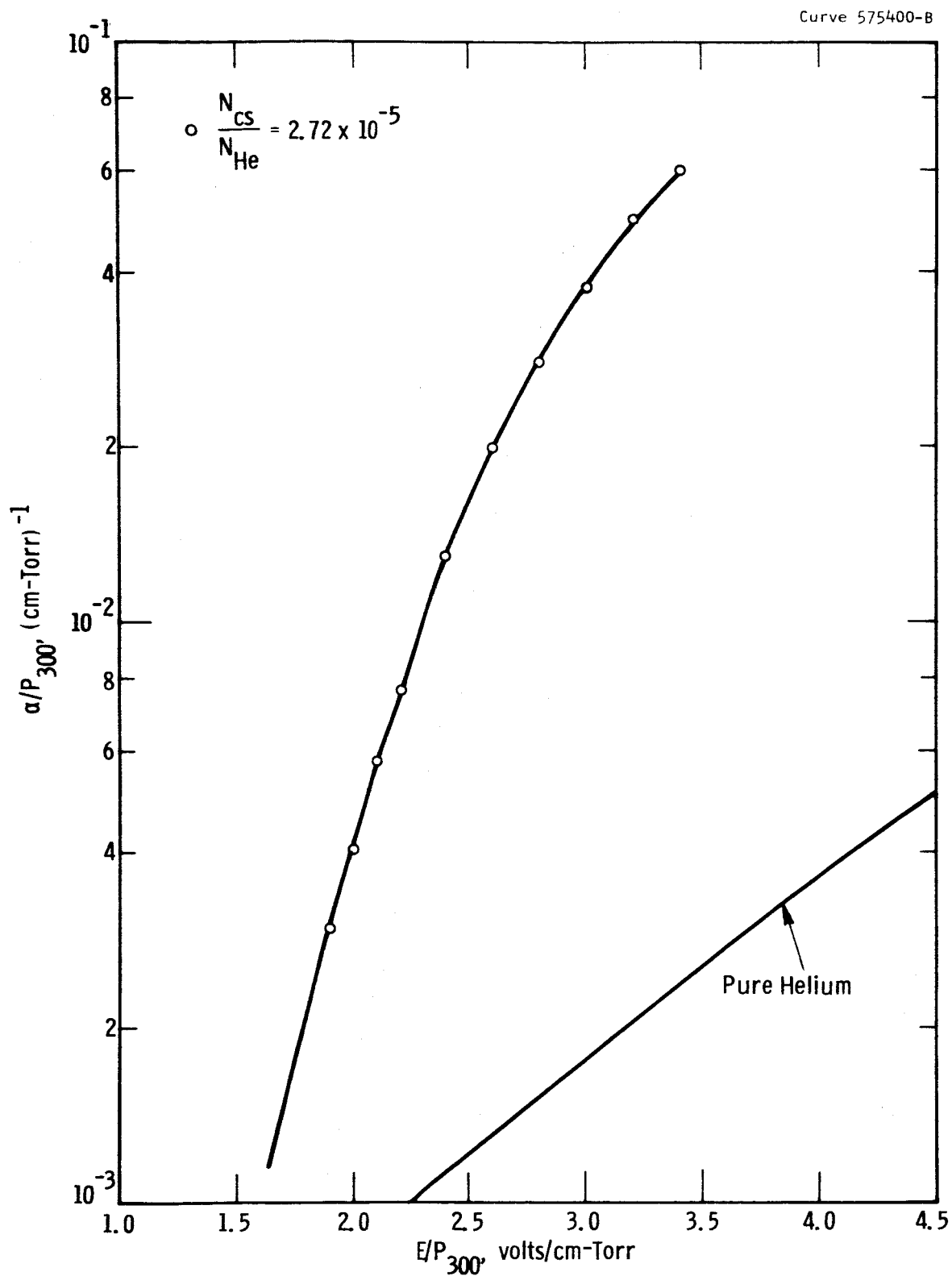


Figure 7 α/P_{300} vs. E/P_{300} for $N_{Cs}/N_{He} = 2.72 \times 10^{-5}$. Also shown for comparison is α/P_{300} vs. E/P_{300} for pure helium, taken from the work of Chanin and Rork (reference 13).

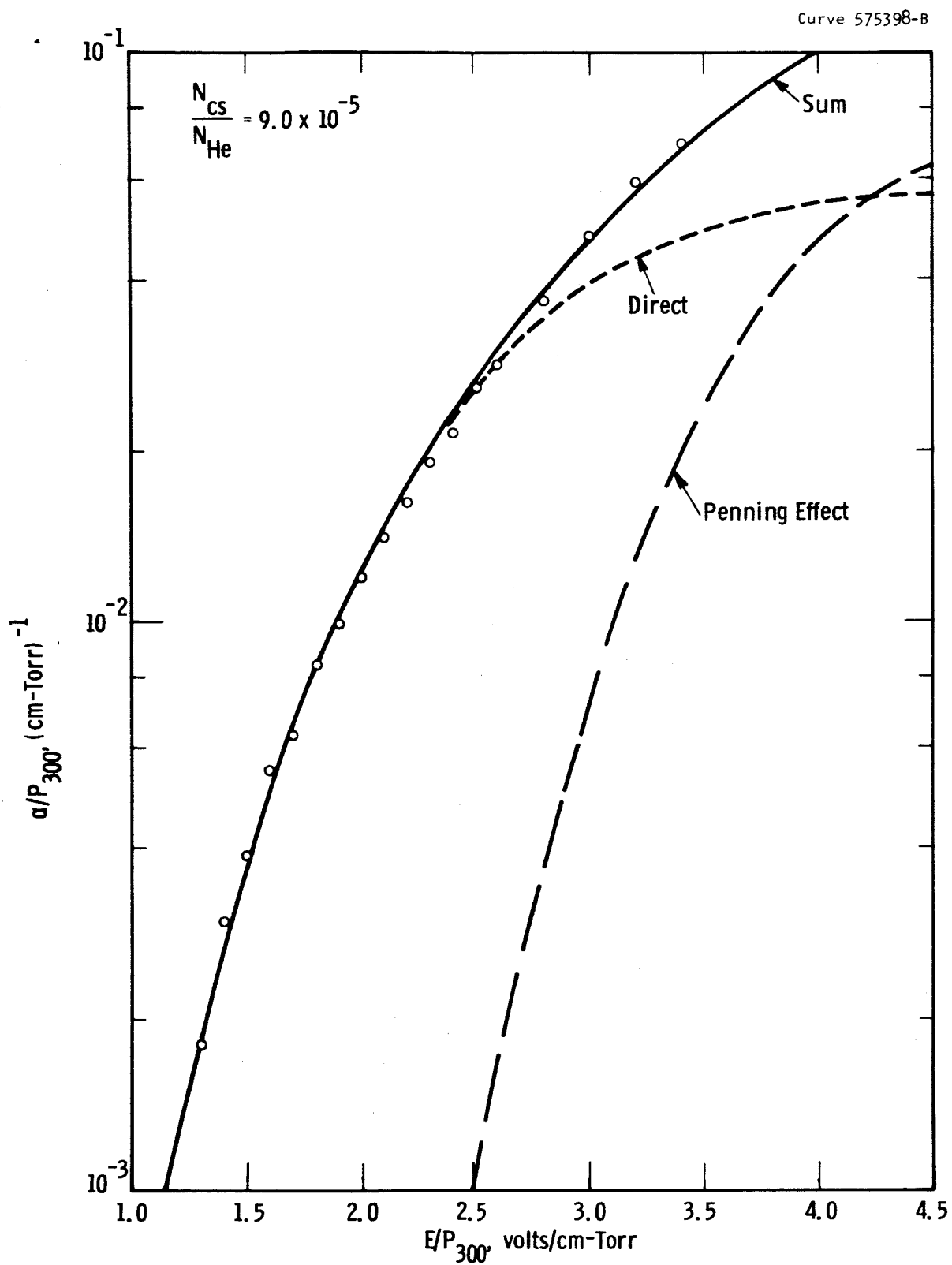


Figure 8 α/P_{300} vs. E/P_{300} for $N_{Cs}/N_{He} = 9.0 \times 10^{-5}$. The points are measured values. The solid curve is calculated using the excitation cross section shown in Fig. 9. The dashed curves show the contribution of direct ionization and Penning effect ionization to the total.

Curve 575395-A

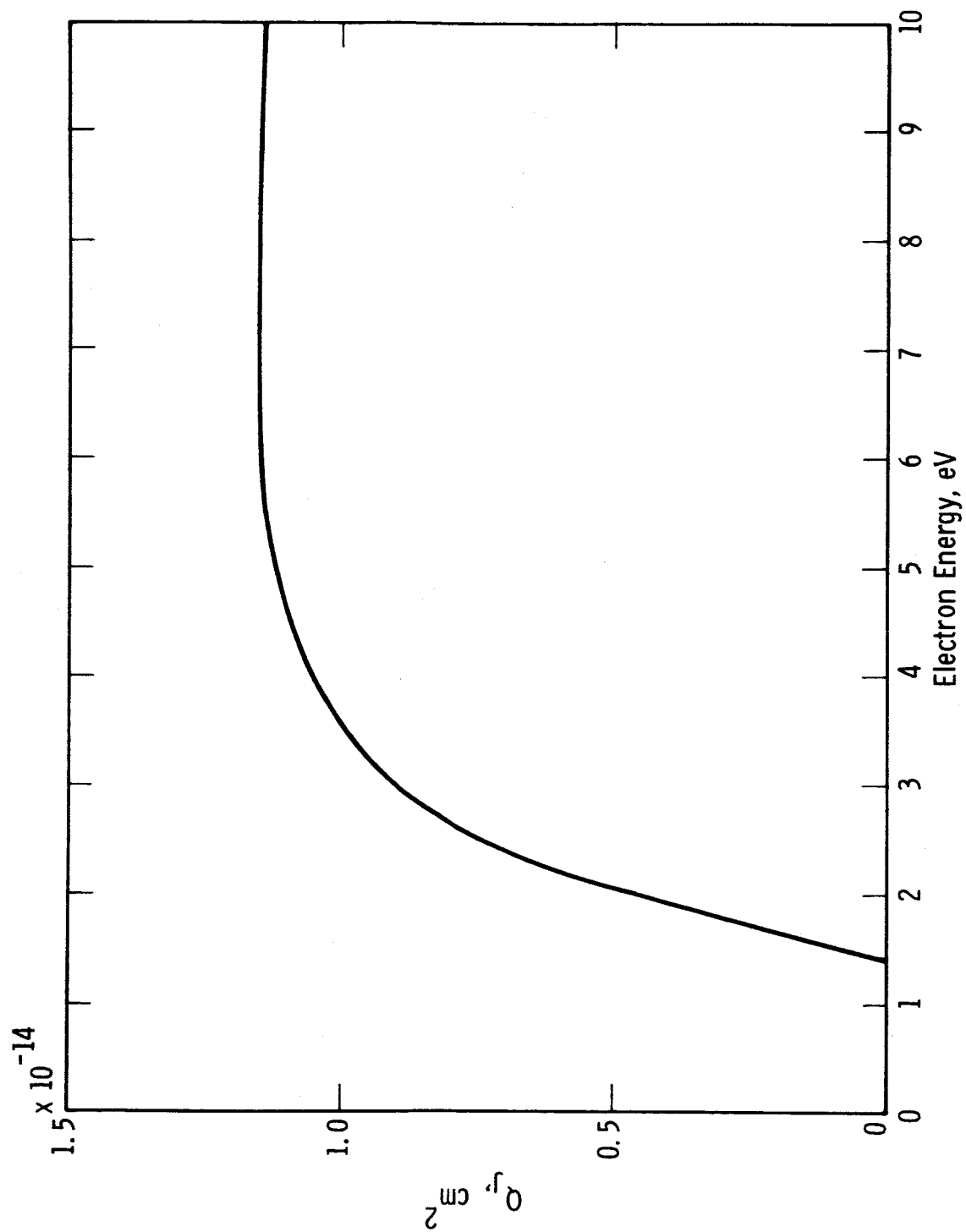


Figure 9 Cesium excitation cross section as a function of electron energy.

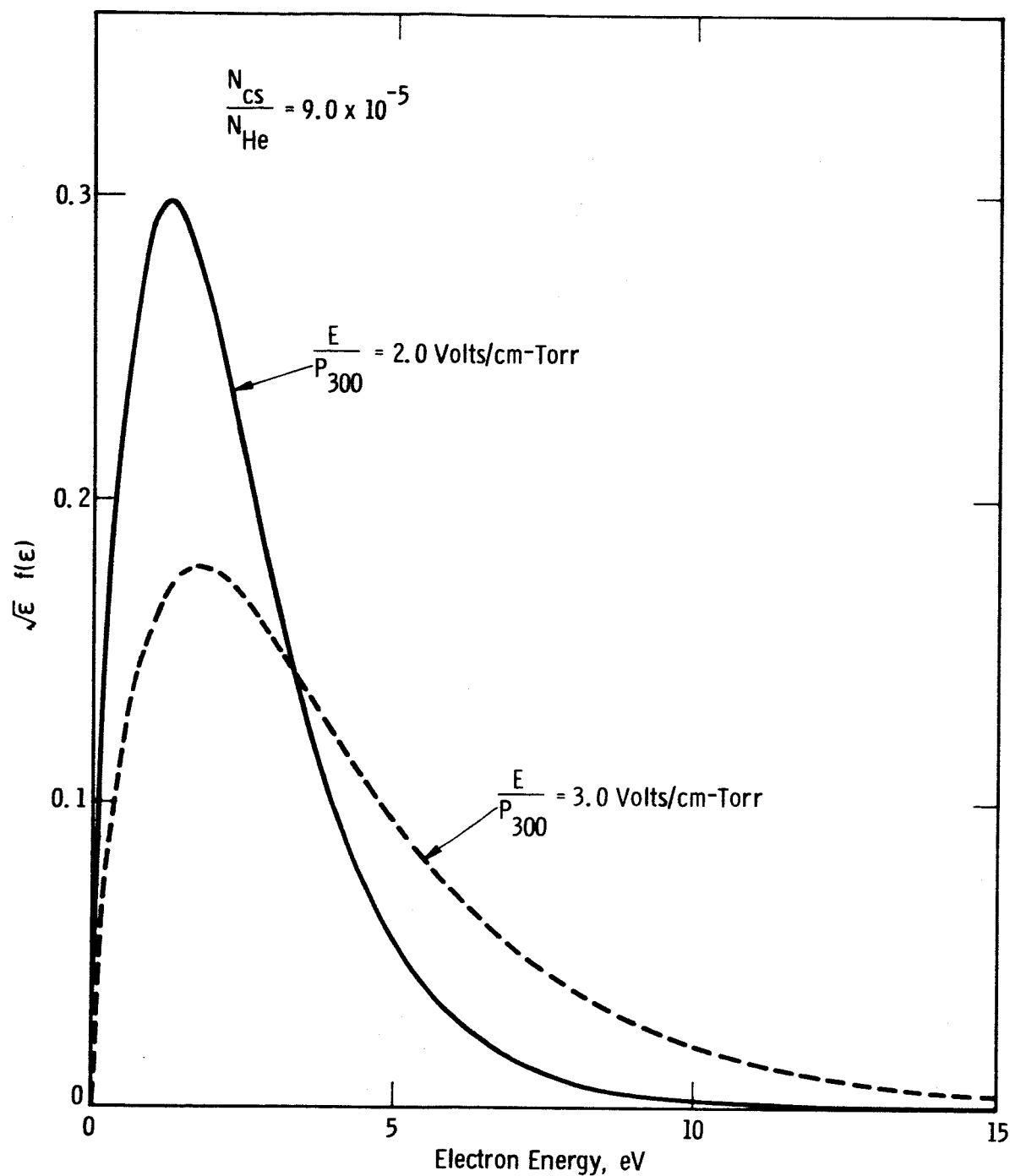


Figure 10 Electron energy distribution functions for two values of E/P_{300} . Also shown for comparison is a Maxwellian distribution function (dotted curve) with a peak energy equal to that of the calculated distribution function for $E/P_{300} = 3.0$ volts/cm-torr.

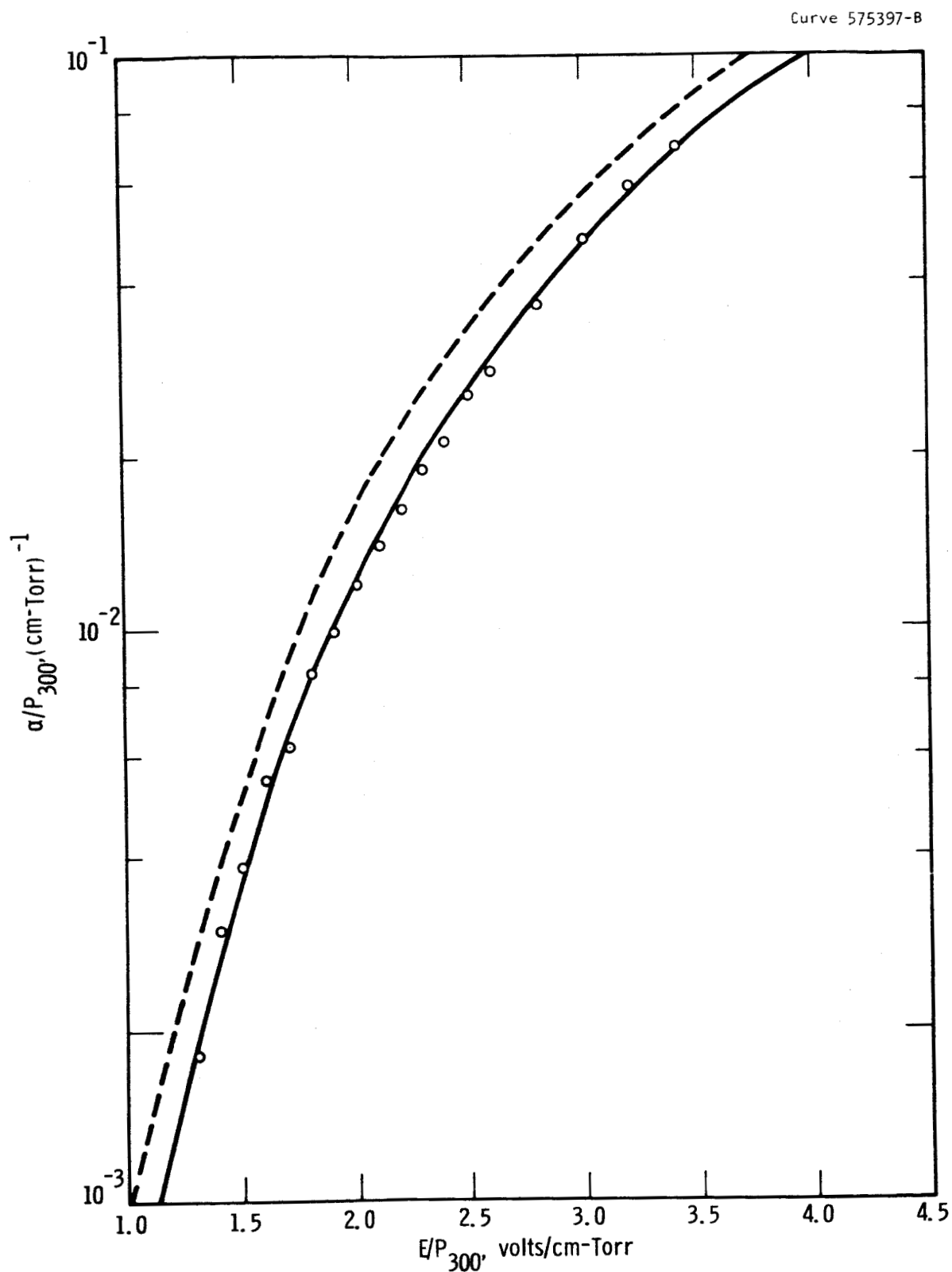


Figure 11

Comparison of α/p_{300} calculated using two different assumed cross sections with measured values. The solid curve is based on the cross section shown in Fig. 9, while the dashed curve is based on a cross section with similar shape but some 20% smaller in magnitude. The dashed curve is clearly not a good fit to experiment, indicating the sensitivity with which the cross section may be determined.

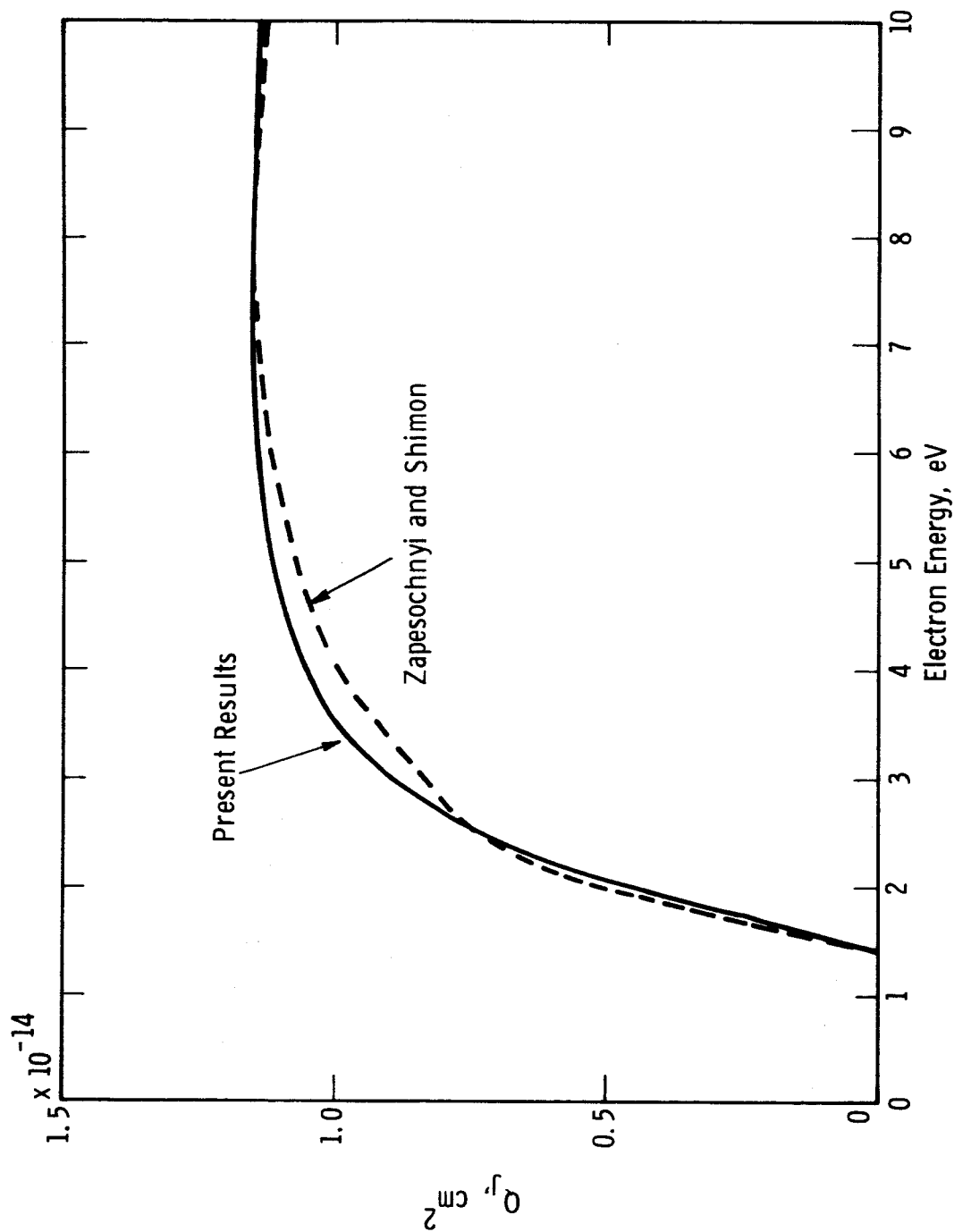


Figure 12 Comparison of the cesium excitation cross section derived from the present work with the excitation function for cesium resonance radiation found by Zapesochnyi and Shimon (reference 22). The Zapesochnyi and Shimon curve is normalized to fit the present curve at 8 eV.

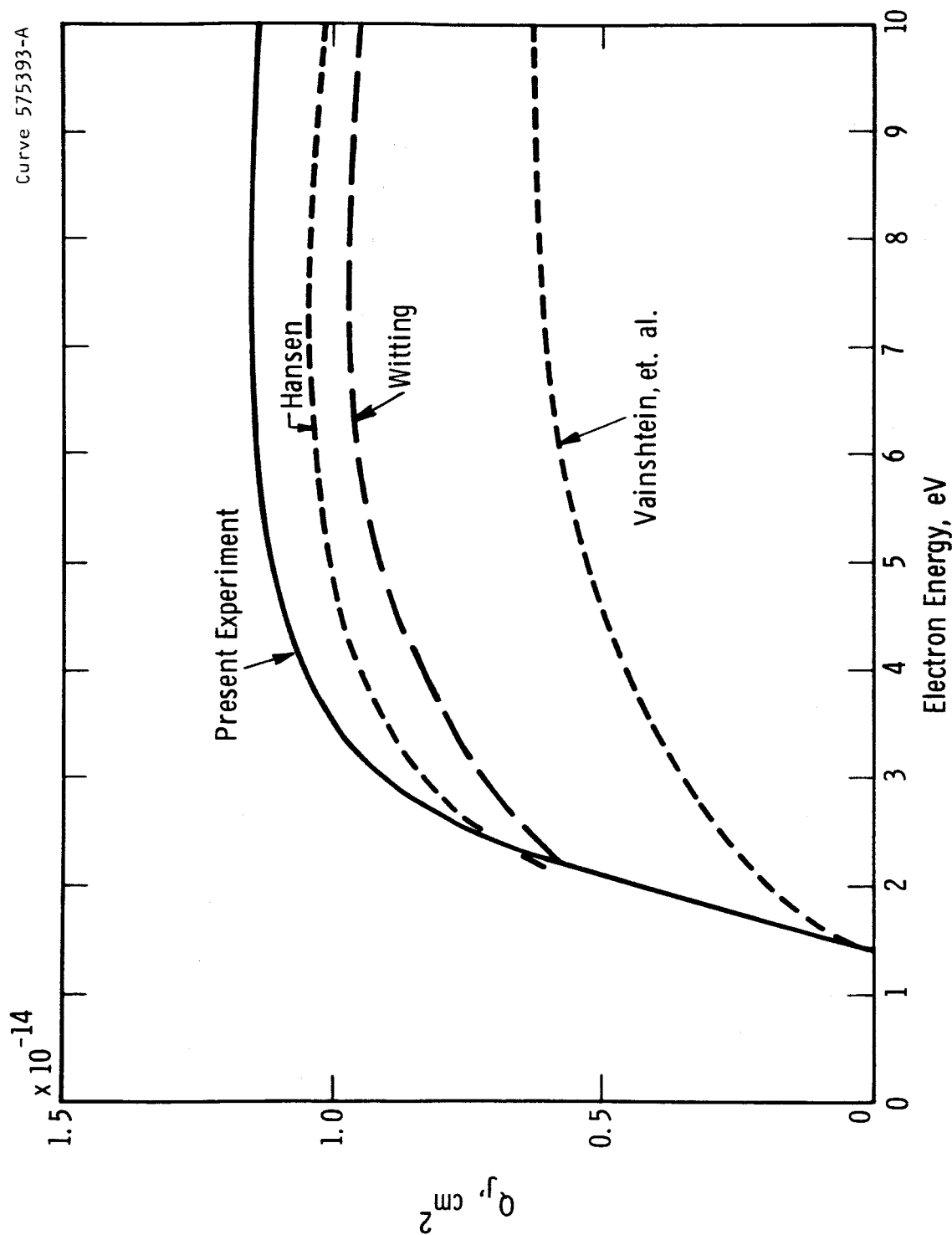


Figure 13 Comparison of theoretical and experimental cesium excitation cross sections. The dashed curves are theoretical calculations by Hansen (reference 23), Witting (reference 24), and Vainshtein, et. al. (reference 25). The solid curve is the experimental cross section derived from the present work.